Journal of Solid State Chemistry 184 (2011) 1581–1590

Contents lists available at ScienceDirect

Journal of Solid State Chemistry

journal homepage: www.elsevier.com/locate/jssc

pH- and metal-dependent structural diversity from mononuclear to two-dimensional polymers based on a flexible tricarboxylate ligand

Chengjuan Li [a], Yanqiang Peng [a], Suna Wang [a,b,*], Xianxi Zhang [a], Yizhi Li [b], Jianmin Dou [a,**], Dacheng Li [a]

[a] School of Chemistry and Chemical Engneering, Liaocheng University, Liaocheng 252059, PR China
[b] State Key Laboratory of Coordination Chemistry, Nanjing 210093, PR China

ARTICLE INFO

Article history:
Received 11 January 2011
Received in revised form
15 April 2011
Accepted 17 April 2011
Available online 27 April 2011

Keywords:
Crystal engineering
Flexible tricarboxylate ligand
pH-dependent
Weak interactions
Topology

ABSTRACT

Six complexes based on a flexible tripodal ligand H_3TTTA (2,2′,2″-[1,3,5-triazine-2,4,6-triyltris(thio)]-tris-acetic acid) have been hydrothermally synthesized and structurally characterized. X-ray single-crystal diffractions reveal that they have rich structural chemistry: mononuclear, $[Zn(HTTTA)(2,2'\text{-bpy})(H_2O)_3]_n$ (**1**); dimeric metallamacrocycle, $[Zn(HTTTA)(2,2'\text{-bipy})(H_2O)]_n$ (**2**) and $[Cd(HTTTA)(2,2'\text{-bipy})(H_2O)\cdot H_2O]_n$ (**3**); two-dimensional networks with binodal (3,6)-connected CdI_2 topology based on linear trinuclear $M_3(\mu^2\text{–}CO^2)_4(\mu_2\text{–}CO_2)_2$ SBUs (Secondary Building Units), $[M_3(TTTA)_2(2,2'\text{-bipy})_2(H_2O)_m\cdot nH_2O]_n$ (M=Zn·**4**, m=0, n=4; Cd·**5** and Mn·**6**, m=2; n=2). The value of pH and the metal ions has large influences on the resulting structures. The flexible tricarboxylic acid exhibits four coordination modes from monodentate to μ^6-bridge. Fluorescence and magnetic properties of the complexes have also been investigated in details.

1. Introduction

Supramolecular coordination assemblies attract much interest in recent years, stemming from the potential applications in the areas including gas storage, molecular sieves, ion-exchange, catalysis, magnetism and optoelectronics, as well as their intriguing variety of architectures and topologies, such as molecular grids, bricks, herringbones, ladders, rings, boxes, diamondoids and honeycombs [1–16]. Of great interest is the construction of supramolecular architectures based on rigid or flexible carboxylic acid ligands [17–27]. Rigid ligands with comparably predictable coordination conformations are also employed in predesigned syntheses. Flexible ones, however, can adopt different conformations to decrease the geometric constrain and steric hindrance, so may form unpredictable intriguing topologies and properties. In addition, various kinds of intermolecular weak interactions, such as O–H···O (N) hydrogen bonds, weak C–H···X (X=O, N, π) and $\pi\cdots\pi$ stacking interactions, are always observed [28–36]. They can cooperate with metal–ligand coordination bonding, leading to interesting supramolecular architectures.

We are interested in the latter and their extended structures. Systematic investigation has been made on the coordination chemistry of a series of tripodal acid ligands containing the $-OCH_2-$, $-NHCH_2-$ and amide groups [37–40]. In our recent manuscript, the lanthanide chemistry of H_3TTTA ligand (2,2′,2″-[1,3,5-triazine-2,4,6-triyltris(thio)]tris-acetic acid) with $-SCH_2-$ group has revealed that three types of structures from three-dimensional networks, one-dimensional chains to metallamacrocycle molecules are observed from light metal ions to heavy ones [41]. The synergistic effect of lanthanide contraction and flexible tripodal ligands should be responsible for the progressive change of these complexes.

For further investigation on coordination chemistry of this ligand with transition metal centers, six complexes were obtained: mononuclear, $[Zn(HTTTA)(2,2'\text{-bipy})(H_2O)_3]_n$ (**1**); metallamacrocycles, $[Zn(HTTTA)(2,2'\text{-bipy})(H_2O)]_n$ (**2**) and $[Cd(HTTTA)(2,2'\text{-bipy})(H_2O)\cdot H_2O]_n$ (**3**); two-dimensional binodal (3,6)-connected CdI_2 networks, $[M_3(TTTA)_2(2,2'\text{-bipy})_2(H_2O)_m\cdot nH_2O]_n$ (M=Zn·**4**, m=0, n=4; Cd·**5** and Mn·**6**, m=2; n=2). The multicarboxylic acid exhibits different deprotonation modes ($HTTTA^{2-}$ and $TTTA^{3-}$) and coordination conformations (monodentate, bisdentate and μ^6-bridge). For mono- and metallamacrocycle complexes, the non-covalent interactions between the molecules induce different packing modes to form diverse supramolecular networks. Fluorescence properties of these complexes have been also investigated.

2. Experimental section

2.1. General methods

The H_3TTTA ligand was prepared according to the previous procedure [40]. All the other reagents were commercially

* Corresponding author at: School of Chemistry and Chemical Engneering, Liaocheng University, Liaocheng 252059, PR China. Fax: +86 635 8239001.
** Corresponding author.
E-mail addresses: wangsuna@lcu.edu.cn (S. Wang), jmdou@lcu.edu.cn (J. Dou).

0022-4596/$ - see front matter © 2011 Elsevier Inc. All rights reserved.
doi:10.1016/j.jssc.2011.04.029

Table 1
Crystal data and refinement of the complexes.

Complex	**1**	**2**	**3**
Empirical formula	$C_{19}H_{21}N_5O_9S_3Zn$	$C_{38}H_{34}N_{10}O_{14}S_6Zn_2$	$C_{38}H_{38}N_{10}O_{16}S_6Cd_2$
Formula weight	624.96	1177.85	1307.94
Space group	$P21/n$	$C2/c$	$C2/c$
a (Å)	7.6656(10)	20.733(2)	21.796(11)
b (Å)	33.813(4)	10.5492(9)	10.584(5)
c (Å)	10.403(2)	21.9589(18)	22.132(11)
α (deg.)	90.00	90.00	90.00
β (deg.)	111.586(2)	104.089(2)	108.221(8)
γ (deg.)	90.00	90.00	90.00
V (Å^3)	2507.5(7)	4658.4(7)	4849.55(3)
Z	4	4	4
$D_{calcd.}$ (g cm^{-3})	1.655	1.679	1.791
μ (mm^{-1})	1.289	1.376	1.215
$R1$, $wR2$[a] [$I>2\sigma(I)$]	0.0347, 0.0819	0.0360, 0.0688	0.0785, 0.2179
GOF	1.007	1.019	1.069
Complex	**4**	**5**	**6**
Empirical formula	$C_{38}H_{36}N_{10}O_{16}S_6Zn_3$	$C_{38}H_{36}N_{10}O_{16}S_6Cd_3$	$C_{38}H_{36}N_{10}O_{16}S_6Mn_3$
Formula weight	1277.24	1418.33	1245.95
Space group	$P-1$	$P-1$	$P-1$
a (Å)	8.883(3)	9.3334(7)	9.4300(6)
b (Å)	11.713(4)	11.0008(8)	10.7611(7)
c (Å)	12.813(4)	13.0536(5)	13.0175(8)
α (deg.)	111.027(4)	108.19 (4)	107.80(5)
β (deg.)	108.443(4)	107.53 (3)	108.68(3)
γ (deg.)	92.013(5)	94.23 (6)	93.26(2)
V (Å^3)	1163.7(7)	1193.01(2)	1173.80(2)
Z	1	1	1
$D_{calcd.}$ (g cm^{-3})	1.823	1.974	1.763
μ (mm^{-1})	1.886	1.669	1.144
$R1$, $wR2$[a] [$I>2\sigma(I)$]	0.0582, 0.1412	0.0532, 0.0937	0.0686, 0.1506
GOF	0.943	1.040	1.090

[a] $R_1=\sum\||F_o|-|F_c|\|/|F_o|$, $wR_2=[\sum w(\sum F_o^2-F_c^2)^2/\sum w(F_o^2)^2]^{1/2}$.

Table 2
Geometrical parameters of hydrogen bonds in the complexes.

D–H···A	d(H···A)	d(D···A)	∠(DHA)	Symmetry codes
Complex 1				
O(2W)–H(2WA)···O(2)	2.06	2.691(3)	130.2	
O(6)–H(6)···O(4)[a]	1.76	2.573(3)	168.9	$x-1/2, -y+3/2, z+1/2$
O(2W)–H(2WB)···O(4)[b]	1.93	2.691(3)	147.6	$-x+2, -y+2, -z+1$
O(3W)–H(3WA)···O(3)[b]	2.17	2.762(3)	126.2	$-x+2, -y+2, -z+1$
O(3W)–H(3WB)···N(3)[c]	2.38	2.949(3)	124.9	$-x+2, -y+2, -z+2$
O(1W)–H(1WB)···O(3)[d]	2.04	2.802(3)	148.6	$-x+1, -y+2, -z+1$
Complex 2				
O(1W)–H(1WA)···O(2)[d]	1.97	2.755(3)	152.8	$-x+1, -y+2, -z+1$
O(1W)–H(1WA)···O(1)[a]	1.94	2.784(3)	172.0	$-x, -y, -z$
O(1W)–H(1WC)···O(5)[b]	2.22	2.783(3)	124.2	$x, y-1, z$
O(3)–H(3)···O(2)	1.79	2.602(3)	169.7	
C(17)–H(17)···O(4)[c]	2.68	3.290(4)	123.5	$-x+1/2, y+1/2, -z+1/2$
C(6)–H(6B)···N(2) [d]	2.41	3.377(4)	171.0	$-x+1/2, y-1/2, -z+1/2$
C(13)–H(13)···O(6) [e]	2.64	3.277(5)	126.4	$x+1/2, y-1/2, z$
Complex 3				
O(3)–H(3)···O(2)	1.89	2.640(10)	150.9	
O(2W)–H(2WC)···O(4)	2.11	2.787(14)	136.1	
O(1W)–H(1WA)···O(6)[a]	2.03	2.702(9)	135.3	$x, y-1, z$
O(1W)–H(1WA)···O(1)[b]	2.34	3.037(9)	139.3	$-x+2, -y+1, -z+2$
O(1W)–H(1WB)···O(2W)[c]	2.01	2.850(14)	167.2	$x, -y+1, z+1/2$
O(2W)–*H*(2WB)···O(5)[d]	2.51	2.934(17)	111.9	$-x+2, y-1, -z+3/2$
Complex 4				
O(1W)–H(1WA)···O(2W)[a]	2.33	3.005(6)	137.0	$x, y, z+1$
O(1W)–H(1WC)···O(6)[b]	2.33	2.847(4)	119.3	$-x, -y+1, -z+1$
O(2W)–H(2WD)···O(1W)[c]	2.45	3.028(6)	125.5	$-x+1, -y+1, -z+1$

Table 2 (*continued*)

D–H···A	d(H···A)	d(D···A)	∠(DHA)	Symmetry codes
Complex 5				
O(1W)–H(1WA)···O(6) [a]	1.96	2.648(6)	137.1	$x+1, y, z$
O(2W)–H(2WC)···O(1W)[b]	2.47	2.951(6)	116.6	$-x+1, -y+2, -z+1$
O(2W)–H(2WD)···O(1)[c]	2.45	3.043(6)	127.8	$-x+1, -y+1, -z+1$
Complex 6				
O(1W)–H(1WA)···O(6)[a]	2.61	3.108(5)	118.9	$x+1, y, z$
O(2W)–H(2WC)···O(1W)[a]	1.98	2.747(5)	150.3	$x, y-1, z$
O(2W)–H(2WD)···O(1)	2.19	2.966(5)	150.9	

available and used as purchased. The elemental analysis was carried out with a Perkin-Elmer 240C elemental analyzer, at the Center of Materials Analysis, Nanjing University. The FT-IR spectra were recorded from KBr pellets in the range of 4000–400 cm^{-1} on a VECTOR 22 spectrometer. Thermal analyses were performed on a TGA V5.1A Dupont 2100 instrument from room temperature to 700 °C with a heating rate of 10 °C/min under flowing nitrogen, and the data are consistent with the structures. The emission/excitation spectra were recorded on a Hitachi 850 fluorescence spectrophotometer. Magnetic measurements were carried out on a Quantum Design MPMS-5XL SQUID system in a field 2 KOe.

2.2. Syntheses of the complexes

2.2.1. $[Zn(HTTTA)(2,2'\text{-bipy})(H_2O)_3]_n$ (**1**) and $[Zn_2(HTTTA)_2(2,2'\text{-bipy})_2(H_2O)_2]$ (**2**)

A mixture of H_3TTTA (0.010 g, 0.025 mmol), 2,2′-bipy (0.004 g, 0.025 mmol), $Zn(OAc)_2 \cdot 6H_2O$ (0.011 g, 0.05 mmol) with 10 mL H_2O was placed in a Parr Teflon-lined stainless steel vessel and heated to 80 °C for 24 h. Then the reaction system was cooled to room temperature slowly and colorless block crystals of **1** and **2** were obtained. After filtration, the crystals were washed with water and dried in air.

2.2.2. $[Zn_2(HTTTA)_2(2,2'\text{-bipy})_2(H_2O)_2]$ (**2**)

A mixture of H_3TTTA (0.010 g, 0.025 mmol), 2,2′-bipy (0.008 g, 0.05 mmol), $Zn(OAc)_2 \cdot 6H_2O$ (0.011 g, 0.05 mmol) with 10 mL H_2O was placed in a Parr Teflon-lined stainless steel vessel and heated to 80 °C for 24 h. Then the reaction system was cooled to room temperature slowly and colorless block crystals of **2** were obtained. After filtration, the crystals were washed with water and dried in air (Yield 50% based on $Zn(OAc)_2 \cdot 6H_2O$). $C_{38}H_{34}N_{10}O_{14}S_6Zn_2$ (1177.85): calcd. C 38.71, H 2.89, N 11.89; found C 38.89, H 3.02, N 11.66. IR (KBr pellet): 3424(w), 1743(m), 1629(m), 1581(m), 1472(s), 1395(w), 1272(m), 1215(w), 852(m), 771(m) cm^{-1}.

2.2.3. $[Cd_2(HTTTA)_2(2,2'\text{-bipy})_2(H_2O)_2 \cdot 2H_2O]_n$ (**3**)

A mixture of TTTA (0.010 g, 0.025 mmol), 2,2′-bipy (0.008 g, 0.05 mmol), $Cd(OAc)_2 \cdot 6H_2O$ (0.013 g, 0.05 mmol) with 10 mL H_2O was placed in a Parr Teflon-lined stainless steel vessel and heated to 80 °C for 24 h. Then the reaction system was cooled to room temperature slowly and colorless block crystals of **5** were obtained. After filtration, the crystals were washed with water and dried in air. (Yield 58% based on $Cd(OAc)_2 \cdot 6H_2O$). $C_{38}H_{38}N_{10}O_{16}S_6Cd_2$ (1307.94): calcd. C 34.86, H 2.91, N 10.70; found C 34.96, H 3.02, N 10.56. IR (KBr pellet): 3427(m,br), 2900(w), 1722(v), 1591(m), 1481(s), 1439(w), 1396(m), 1270(m), 1229(m), 1170(w), 847(m,), 769(m) cm^{-1}.

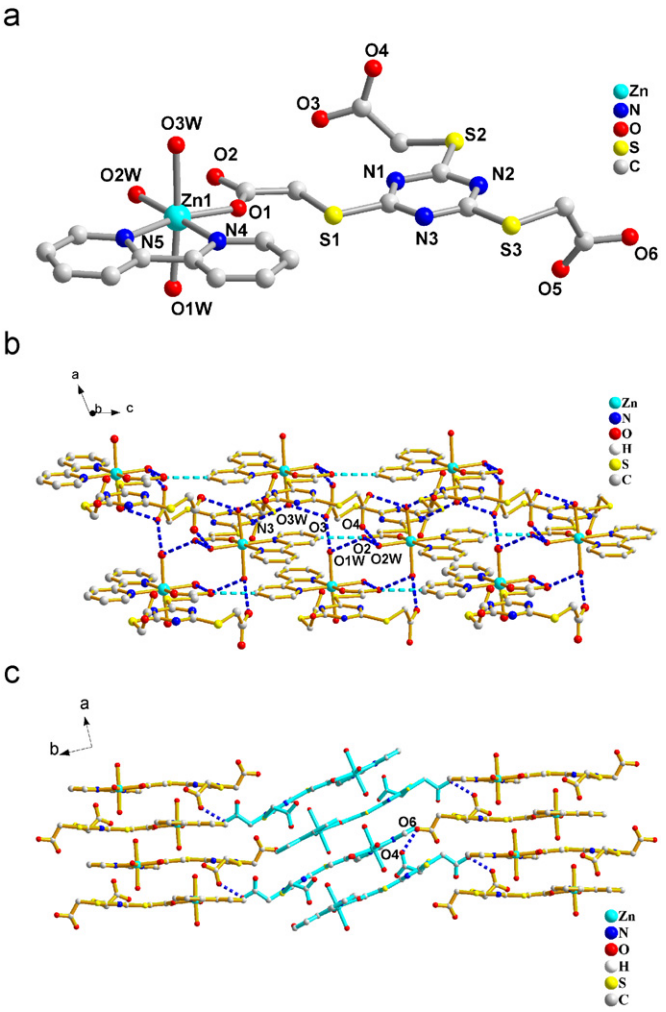

Fig. 1. (a) View of the coordination environment of Zn(II) ion in **1**. (Hydrogen atoms are omitted for clarity.) (b) View of the two-dimensional layer along the *ac* plane, showing the O–H···O and O–H···N hydrogen bonding interactions between the mononuclear units. (c) View of the three-dimensional structure along the *c*-axis, showing the O–H···O and C–H···O interactions.

2.2.4. $[Zn_3(TTTA)_2(2,2'\text{-bipy})_2 \cdot 4H_2O]_n$ (**4**)

H_3TTTA (0.010 g, 0.025 mmol) was dissolved in 10 mL H_2O, and the pH value is adjusted to 4.6 with NaOH. After 2,2′-bipy (0.008 g, 0.05 mmol) and $Zn(OAc)_2 \cdot 6H_2O$ (0.013 g, 0.05 mmol) were added, the whole mixture was placed in a Parr Teflon-lined stainless steel vessel and heated to 80 °C for 24 h. Then the reaction system was cooled to room temperature slowly and colorless block crystals of **4** were obtained. After filtration, the crystals were washed with

water and dried in air. (Yield 70% based on $Zn(OAc)_2 \cdot 6H_2O$). $C_{38}H_{36}N_{10}O_{16}S_6Zn_3$ (1277.24): calcd. C 35.70, H 2.82, N 10.96; found C 35.62, H 2.72, N 11.04. IR (KBr pellet): 3448(m,br), 2978(vw), 1611(s), 1491(s), 1475(s), 1443(m), 1406(s), 1364(m), 1270(m), 1246(m), 1211(m), 856(w), 770(w), 680(vw) cm^{-1}.

2.2.5. $[Cd_3(TTTA)_2(2,2'\text{-bipy})_2(H_2O)_2 \cdot 2H_2O]_n$ (**5**)

H_3TTTA (0.010 g, 0.025 mmol) was dissolved in 10 mL H_2O, and the pH value is adjusted to 4.6 with NaOH. After 2,2′-bipy (0.008 g, 0.05 mmol) and $Cd(OAc)_2 \cdot 6H_2O$ (0.013 g, 0.05 mmol) were added, the whole mixture was placed in a Parr Teflon-lined stainless steel vessel and heated to 80 °C for 24 h. Then the reaction system was cooled to room temperature slowly and colorless block crystals of **5** were obtained. After filtration, the crystals were washed with water and dried in air. (Yield 71% based on $Cd(OAc)_2 \cdot 6H_2O$). $C_{38}H_{36}N_{10}O_{16}S_6Cd_3$ (1418.33): calcd. C 32.15, H 2.54, N 9.87; found C 32.30, H 2.66, N 9.75. IR (KBr pellet): 3464(w,br), 1610(s), 1490(s), 1475(s), 1406(s), 1364(m), 1270(m), 1246(m), 1211(m), 856(w), 770(w) cm^{-1}.

2.2.6. $[Mn_3(TTTA)_2(2,2'\text{-bipy})_2(H_2O)_2 \cdot 2H_2O]_n$ (**6**)

A mixture of TTTA (0.010 g, 0.025 mmol), 2,2′-bipy (0.008 g, 0.05 mmol), $Mn(OAc)_2 \cdot 6H_2O$ (0.013 g, 0.05 mmol) with 10 mL H_2O was placed in a Parr Teflon-lined stainless steel vessel and heated to 80 °C for 24 h. Then the reaction system was cooled to room temperature slowly and light yellow block crystals of **6** were obtained. After filtration, the crystals were washed with water and dried in air. (Yield 70% based on $Mn(OAc)_2 \cdot 6H_2O$). $C_{38}H_{36}N_{10}O_{16}S_6Mn_3$ (1245.95): calcd. C 36.60, H 2.89, N 11.24; found C 36.43, H 3.05, N 11.32. IR (KBr pellet): 3384(w,br), 1608(s), 1485(s), 1445(w), 1410(s), 1361(m), 1263(m), 1246(m), 1205(m), 853(w), 772(w), 676(w) cm^{-1}.

2.3. X-ray crystallographic study

Suitable single crystals were selected for indexing and intensity data were measured on a Siemens Smart CCD diffractometer with graphite-monochromated Mo $K\alpha$ radiation (λ=0.71073 Å) at 293 K. The raw data frames were integrated into SHELX-format reflection files and corrected using SAINT program. Absorption corrections based on multiscan were obtained by the SADABS program. The structures were solved with direct methods and refined with full-matrix least-squares technique using the SHELXS-97 and SHELXL-97 programs, respectively [42]. The coordinates of the non-hydrogen atoms were refined anisotropically, and the positions of the H-atoms were generated geometrically, assigned isotropic thermal parameters, and allowed to ride on their parent carbon atoms before the final cycle of refinement. Basic information pertaining to crystal parameters

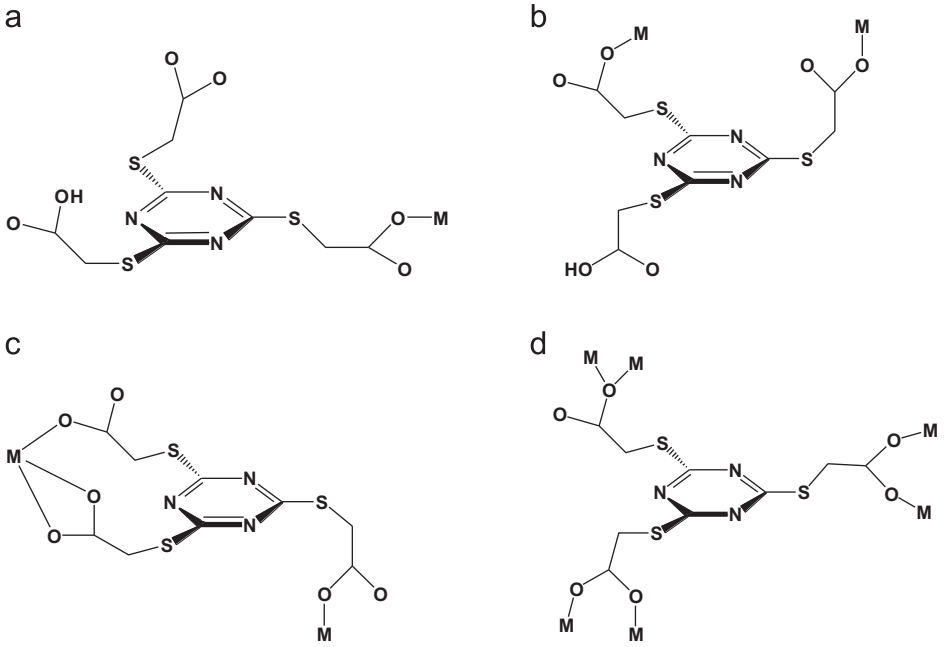

Scheme 1. Deprotonation and coordination conformations of H_3TTTA ligand in the complexes.

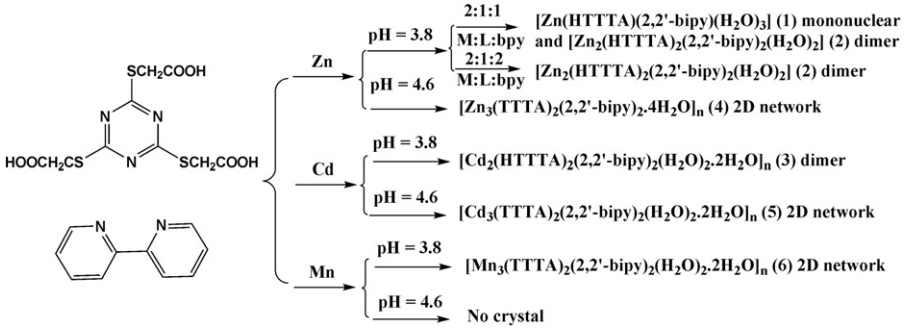

Scheme 2. Syntheses of the complexes.

and structure refinement is summarized in Table 1, and selected bond lengths and angles are listed in Table 2. CCDC 793233(**1**), 787392(**2**), 787393(**3**), 787396(**4**), 787397(**5**), 787395(**6**) for the complexes contain the supplementary crystallographic data for this paper. These data can be obtained free of charge from The Cambridge Crystallographic Data Centre via www.ccdc.cam.ac.uk/data_request/cif.

2.4. Calculation details

Density functional calculations were performed, employing the Gaussian03 suite of programs, at the B3LYP level. The basis set used for C, O, N, S and H atoms was 6–31 G while effective core

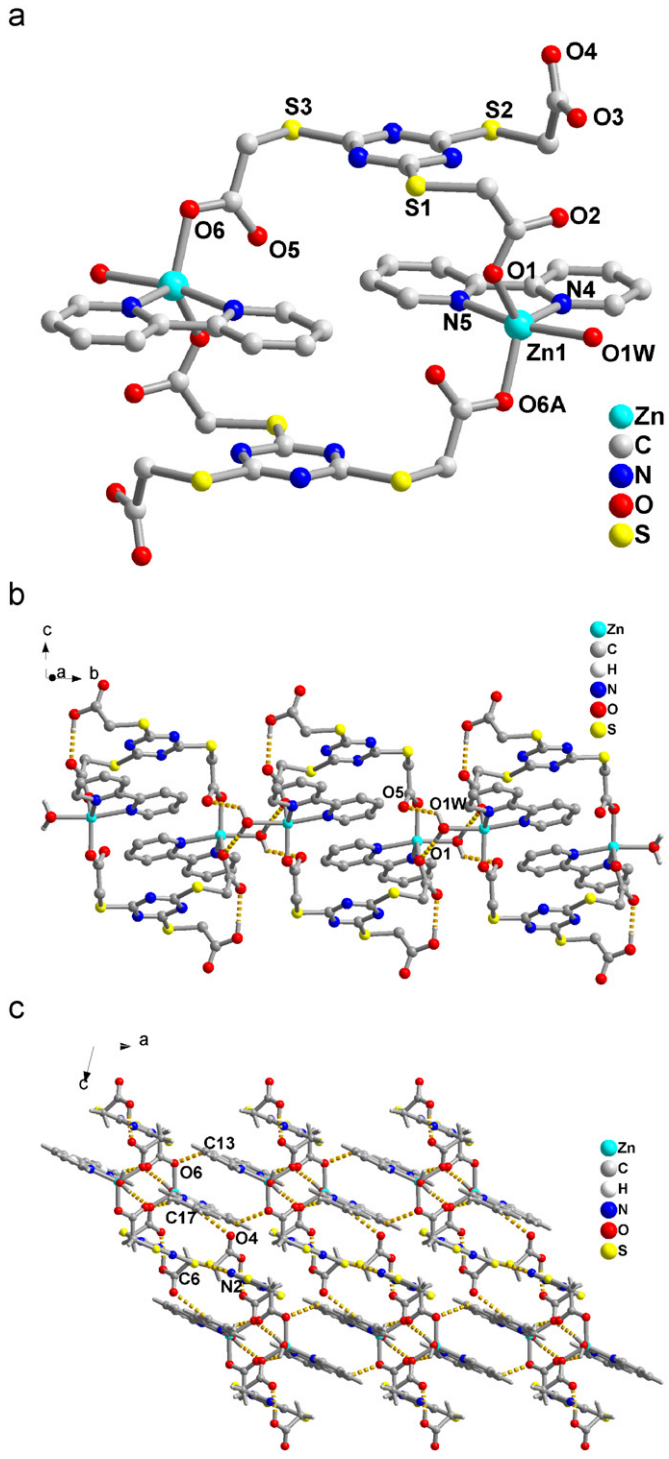

Fig. 2. (a) View of the coordination environment of Zn(II) ion in **2**. Symmetry codes to generate the atoms: *A*, $-x$, $1-y$, $-z$. (b) View of the one-dimensional chain along the c axis with O–H···O hydrogen bonding interactions along the *b*-axis. (c) View of the three-dimensional network connected by C–H···O and C–H···N weak interactions between adjacent chains along the ac plane. (Hydrogen atoms are omitted for clarity.)

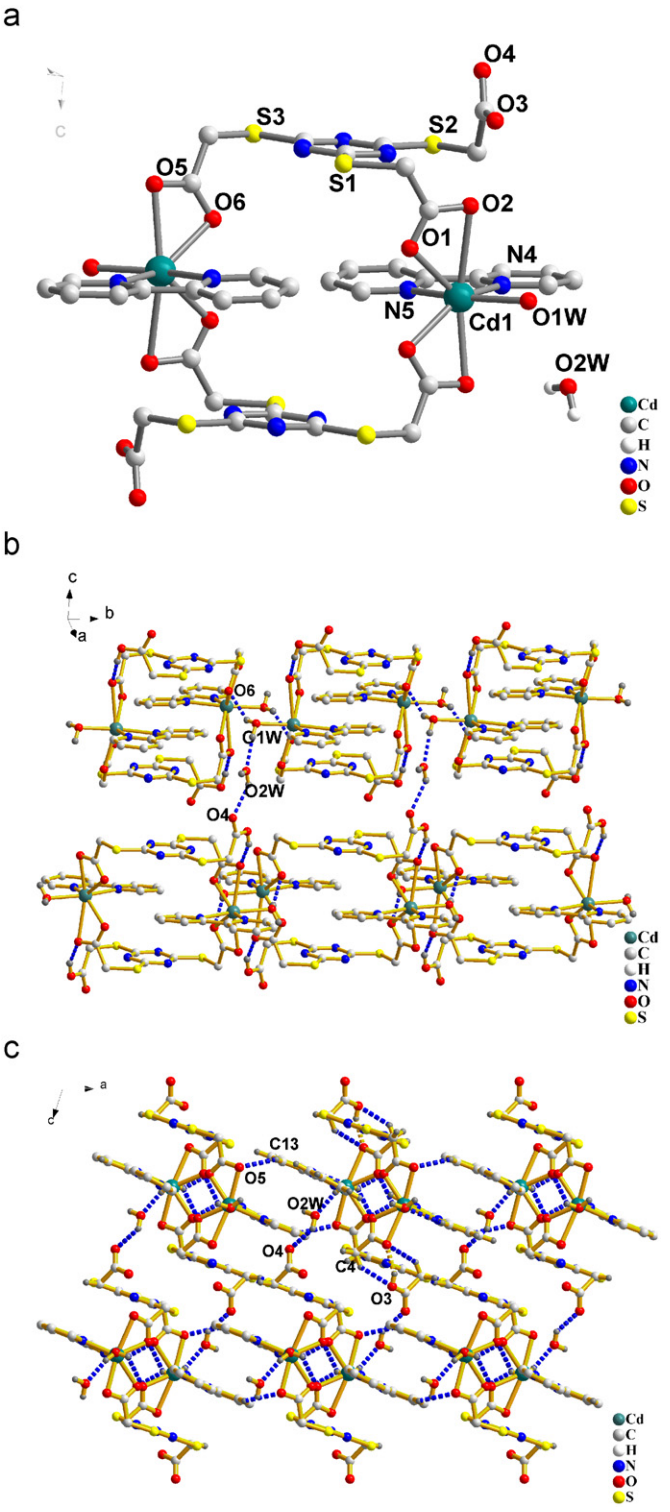

Fig. 3. (a) View of the coordination environment of Cd(II) ion in **3**. Symmetry codes to generate the atoms: *A*, $2-x$, $2-y$, $2-z$. (b) View of the one-dimensional chain along the c axis with O–H···O hydrogen bonding interactions along the *b*-axis. (c) View of the three-dimensional network connected by C–H···O and C–H···N weak interactions between adjacent chains along the ac plane. (Hydrogen atoms are omitted for clarity.)

potentials with a LanL2DZ basis set were employed for transition metals. The contour plots of MOs were obtained with the Gaussview 3.0 graphic program.

3. Results and discussion

3.1. Syntheses

It is well known that generation of supramolecular architectures are governed by the crystallization conditions, such as temperature, solvent, template, guest, concentration and so on. The reactions under different pH values for different metal salts in two kinds of ratio have been carried out. PXRD was measured to confirm the purities of the complexes (see Supporting Information). As can be seen from Scheme 2, the resulting products are largely dependent on the values of pH. For Zn system, the influence is more significant. Within the pH value of 3.8–4.6, low values gave rise to simple structures while high values resulted in complicated ones, which may be related with the deprotonation degrees of the multicarboxylate ligands. Reactions of higher pH values, such as 5.0, may lead to the decomposition of the carboxylate ligand and the hydrolysis of the metal centers.

3.2. Structural description

3.2.1. Mononuclear structure. $[Zn(HTTTA)(2,2'\text{-bpy})(H_2O)_3]_n$ (**1**)

X-ray diffraction indicates complex **1** features a mononuclear molecule. The asymmetric unit is composed of one metal center, one $HTTTA^{2-}$ ligand, one chelating 2,2′-bpy and three coordinated aqua molecules (Fig. 1(a)). The Zn(II) center adopts a six-coordinated geometry. One monodentate carboxylate oxygen atom from $HTTTA^{2-}$ ligand, two nitrogen atoms from chelating 2,2′-bpy molecule as well as one aqua oxygen atom composed the equatorial plane. The other two aqua oxygen atoms occupy the axial positions. The Zn–O and Zn–N bond lengths are in the range of 2.045(2)–2.165(2) Å. The N4–Zn–N5 angle is 77.1°, indicating the octahedral coordination sphere is much distorted. The tripodal ligand is incompletely deprotonated and adopts a simple monodentate mode with one carboxyl group almost coplanar with the central triazine ring (Scheme 1(a)).

Analysis of the supramolecular structure showcases the importance of the non-covalent intermolecular interactions in directing a network topology (Fig. 1(b) and (c)). The aqua molecules O1w, O2w and O3w form strong O–H···O interactions with the carboxylate oxygen atoms O2, O3, O4 and triazine nitrogen atom N3, resulting into two-dimensional layers along the *ac* plane, which is stabilized further through the C–H···O weak interactions between the bpy carbon atom C12 and carboxylate oxygen atom O2. These layers are linked further through O–H···O interactions between the carboxylic oxygen atom O6 and carboxylate oxygen O4, extending the layers into a three-dimensional supramolecular structure.

3.2.2. Dimeric metallamacrocycle. $[Zn_2(HTTTA)_2(2,2'\text{-bipy})_2(H_2O)_2]_n$ (**2**) and $[Cd_2(HTTTA)_2(2,2'\text{-bipy})_2(H_2O)_2\cdot 2H_2O]_n$ (**3**)

As shown in Fig. 2(a), complex **2** is a metallamacrocycle molecule, composed of two metal centers, two $HTTTA^{-}$ ligands, two 2,2′-bpy ligands and two aqua molecules. The Zn(II) center is five-coordinated with two monodentate carboxylate oxygen atoms, two nitrogen atoms of chelating bpy and one water molecule, resulting in much distorted triangular bipyramidal geometry. The incompletely deprotonated ligand acts as a μ^2-bridge, linking two metal centers with the separation of $Zn1\cdots Zn1^{ii}$ (symmetry code: ii, $2-x$, $2-y$, $2-z$.) being 8.59(1) Å.

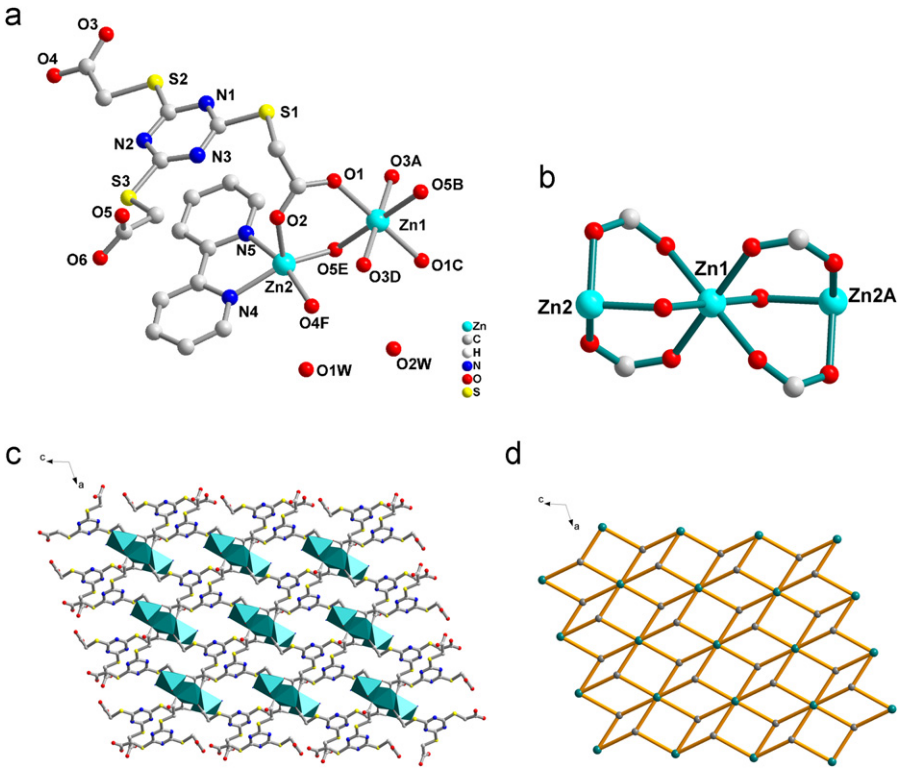

Fig. 4. (a) View of the coordination environments of Zn(II) ions in **4**. Symmetry codes to generate the atoms: A, $1-x$, $-y$, $1-z$; B, $-x$, $-y$, $-z$; C, $1-x$, $-y$, $-z$; D, x, y, $-1+z$; E, $1+x$, y, z; F, x, y, $-1+z$. Hydrogen atoms are omitted for clarity. (b) View of the trinuclear SUBs. Symmetry code: A, $1-x$, $-y$, $-z$; (c) View of the two-dimensional sheet along the ac plane. (d) Scheme representation of (3,6)-connected CdI_2 topology. The $TTTA^{3-}$ ligands and trinuclear SBUs are represented by 3- and 6-connected nodes, respectively.

The neighboring molecules are arranged into 1-D chains along the *b* axis by strong intermolecular hydrogen bonding interactions between the coordinated molecule O1w and the carboxylate oxygen atoms O1 and O5, respectively, in which M_2O_2 rings are formed with the metal–metal separation of 4.740 Å (Fig. 2(b)). Adjacent chains are connected further through weak C–H···O interactions between phen carbon atoms (C13, C17) and carboxylate oxygen atoms (O6, O4), as well as C–H···N interactions between methyl carbon atom C6 and triazine nitrogen atom N2, resulting into a 3D framework (Fig. 2(c)).

The molecule structure of complex **3** is similar to that of complex **2**. Due to the larger radii, Cd(II) ion is six-coordinated by two chelating carboxylate groups, two chelating nitrogen atoms and one aqua molecule (Fig. 3(a)). The bond length of Cd1–O2 is 2.710(2) Å, much longer than other bonds, and the comparable Cd1–O5 and Cd1–O6 bonds suggest the symmetric coordination of the carboxylate group. Thus, the environment around the metal center is much distorted. Additionally, free aqua molecules are observed, which are involved in the weak hydrogen bonding interactions connecting these dimeric molecules into three-dimensional supramolecular architectures (Fig. 3(b) and (c)).

3.2.3. *Two-dimensional complexes. $[M_3(TTTA)_2(2,2'\text{-bipy})(H_2O)_m \cdot nH_2O]_n$ (M=Zn · 4, m=0, n=4; Cd · 5 and Mn · 6, m=2, n=2)*

Complex **4**–**6** exhibit high-dimensional networks. As illustrated in Fig. 4(a), the fundamental unit consists of two crystallographically independent Zn(II) ions. Zn1 is surrounded by six monocarboxylate oxygen atoms from discrete $TTTA^{3-}$ ligands, resulting in octahedral coordination geometry. The Zn–O distances are in the range of 2.233(2)–2.320(3) Å. Zn2 shows a distorted square pyramidal coordination sphere. The equatorial plane is composed of chelating bpy ligand and two monodentate carboxylate oxygen atoms from two $TTTA^{3-}$ ligands. The apical positions are occupied by one carboxylate oxygen atom from $TTTA^{3-}$ ligand. In addition, there are also $\pi\cdots\pi$ stacking interactions between the triazine ring and the bpy ring with the average plane-to-plane separation of 3.54(5) Å.

The tricarboxylate ligand is completely deprotonated. Three arms show significant deviation from the aromatic ring and exhibit different coordination modes: μ^2–η^1:η^1 fashion (each of the carboxylate oxygen atoms coordinates with one metal center); μ^2–η^1:η^1 fashion and μ^2–η^2 (only one carboxylate oxygen atom coordinates with two metal centers). As a result, the whole ligand functions as a μ^6-bridge, linking six metal centers.

The most interesting feature of the complex is the presence of linear $[Zn_3(\mu_2\text{–}O)_2(CO_2)_4]$ SBUs (Fig. 4(b)). Zn1 center is located at the vertex and triply bridged to the central Zn2 by two bidentate carboxylate groups in *syn–syn* conformation and one oxygen atom from the monodentate-bridging group. The Zn1···Zn2 distance is 3.611(2) Å. The assembly of these trinuclear SBUs with $TTTA^{3-}$ ligands leads to a 2D compact and neutral framework along the *ac* plane. Within the sheet, each Zn_3 SBU is connected with other six ones (Fig. 4(c)). Adjacent aromatic rings are separated with the central distance of 3.307 and 3.327 Å, respectively, exhibiting strong $\pi\cdots\pi$ stacking interactions. The free aqua molecule O2w can form O–H···O hydrogen bonds with O1w and the carboxylate oxygen O4, connecting these sheets into a three-dimensional network.

To classify the network, suitable nodes should be confirmed. The Zn_3 SBUs and the geometrical centers of the triazine ring of the $TTTA^{3-}$ ligands can be viewed as six-connected nodes as three-connected nodes, respectively. The 2D layer is composed of 4-gons sharing edges or vertices, corresponding to the well-known (3,6)-connected CdI_2 topology with the short Schäfli symbol of $(4^3)_2(4^6, 6^6, 8^3)$ (Fig. 4(d)) [43]. It is well known that high-dimensional nets with mixed connectivity, such as (3,6)-, (4,6)- and (4,8)-connected architectures, are still quite rare [44–47]. Only several (3,6)-connected structures have been observed in Metal-Organic Frameworks (rutile, pyrite and anatase), other reported examples are inorganic materials (α-PbO_2, γ-ZnO_2, brookite and PrI_2) [4,48–51].

Complex **5** and **6** are isostructural and similar to complex **4**, except the coordination environments of the metal centers (Fig. 5(a) and (b)). In these two cases, two crystallographically independent metal centers both exhibit six-coordinated distorted octahedral coordination environment. As shown in Fig. 5(a), six monocarboxylate oxygen atoms around Cd1 center come from discrete $TTTA^{3-}$ ligands. Cd2 shows a distorted octahedral coordination sphere, with the equatorial plane composed of chelating bpy ligand and two monodentate carboxylate oxygen atoms from two $TTTA^{3-}$ ligands, as well as one carboxylate oxygen atom from the third $TTTA^{3-}$ ligand and one water molecule in the apical positions.

3.2.4. *Structural progression of the complexes*

A structural comparison shows the structural progression of the six complexes. Apparently, pH of the reaction system has large influence on the final products. Higher pH always leads to higher-dimensional structures, which is in agreement with the previous reports [52,53]. It may have control over the deprotonation

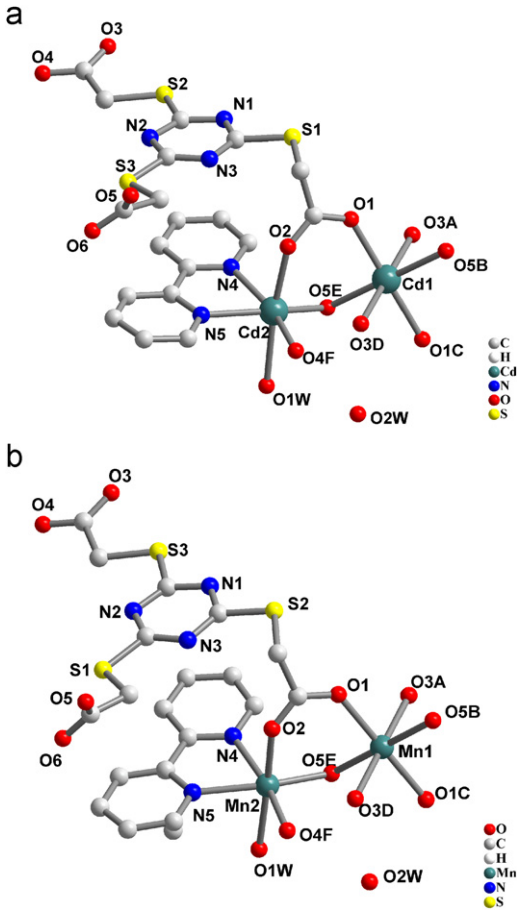

Fig. 5. (a) View of the coordination environments of Cd(II) ions in **5**. Symmetry codes to generate the atoms: A, $2-x$, $1-y$, $2-z$; B, $1-x$, $1-y$, $1-z$; C, $2-x$, $1-y$, $1-z$; D, x, y, $-1+z$; E, $1+x$, y, z; F, x, y, $-1+z$. (b) View of the coordination environments of Mn(II) ions in **6**. Symmetry codes to generate the atoms: A, $1-x$, $1-y$, $1-z$; B, $-x$, $1-y$, $-z$; C, $1-x$, $-y$, $-z$; D, x, y, $-1+z$; E, $1+x$, y, z; F, x, y, $-1+z$. Hydrogen atoms are omitted for clarity.

and thus a higher connectivity of the carboxylate ligand and consequently more complicated high dimensional structure. Additionally, metal centers also demonstrate pH-dependence. The same pH for different metal centers may not often result in the same structures. Depending on the coordination requirement of the metal center and a particular network formation, the flexible ligand can adopt different conformations via bending, stretching, or twisting. A superimposed picture of the ligand in **1–6** will put this into perspective (Table 3 and Fig. 6). The conformational variations can broadly be quantified by two groups of parameters: (i) the dihedral angles between the triazine ring and the three carboxylate groups, α, β and γ; (ii) *syn* or *anti* conformation of the three arms. Moreover, the existence of N, O and S atoms as well as aromatic ring is important to the construction of the supramolecular framework, especially for the low-dimensional ones (mononuclear and dinuclear units). Anyway, these special structures may enrich the frameworks of multicarboxylate system to some extent.

Table 3
Conformational parameters of the H_3TTTA molecule.

Complex	α (deg.)	β (deg.)	γ (deg.)	Conformation
1	9.3	84.4	105.5	*syn, syn, anti*
2	88.9	101.5	90.0	*syn, syn, anti*
3	90.0	77.9	89.9	*syn, syn, anti*
4	119.3	19.7	74.1	*syn, syn, anti*
5	131.1	15.0	70.8	*syn, syn, anti*
6	121.6	13.3	73.8	*syn, syn, anti*

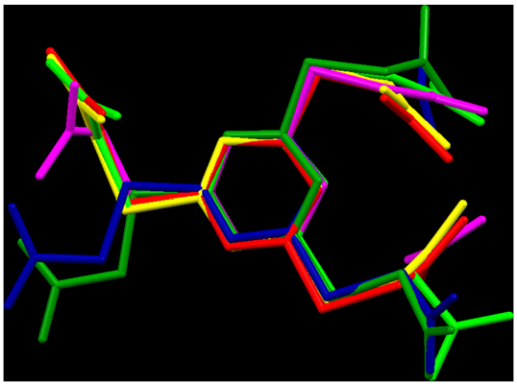

Fig. 6. Overlay of the H_3TTTA acid in the complexes, showing the flexibility of the ligand.

3.3. Properties of these complexes

3.3.1. FT-IR spectra

The IR spectra show features attributable to the carboxylate stretching vibrations of the complexes. For different deprotonation of the ligands, significant signals can be found. For complex **1–3**, the presence of signals in the range of 1760–1680 cm^{-1} indicates the incompletely deprotonation of the ligands, while for **4–6** with the completely deprotonated ligands, these signals are absent. The characteristic bands of carboxylate groups are shown in the range of 1560–1620 cm^{-1} for asymmetric stretching and 1370–1490 cm^{-1} for symmetric stretching. The absorption in the range of 1500–1420 cm^{-1} is characteristic of the C═N and C═C bonds of the aromatic ring. Weak absorptions observed in the range of 2900–2950 cm^{-1} can be assigned to the υ_{CH2} of the ligand. The broad bands at ca. 3300 cm^{-1} are corresponding to the vibration of the water molecules in the complexes.

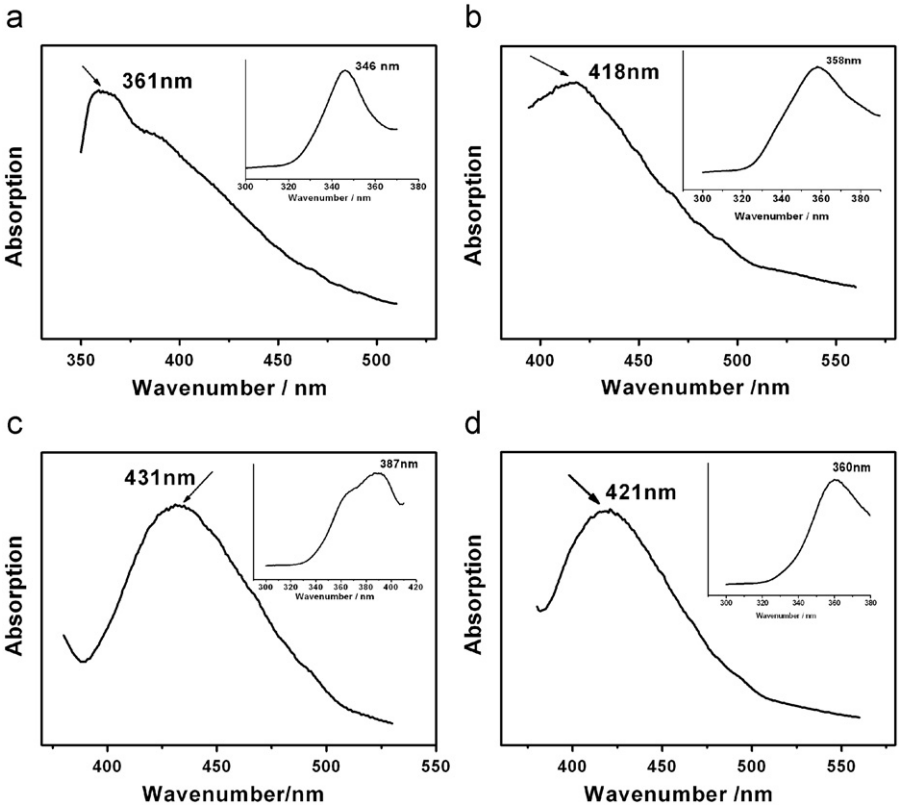

Fig. 7. View of the solid luminescence properties of complex **2** (a), **3** (b), **4** (c) and **5** (d) at room temperature, respectively. Inset: the excitation spectra.

3.3.2. Fluorescence of the complexes

The solid fluorescence properties of these complexes were measured at the ambient temperature. As depicted in Fig. 7, complex **2**–**5** shows strong fluorescent emissions at 361, 418, 431 and 421 nm upon excitation at 346, 358, 387 and 360 nm, respectively. Significant enhancement in the intensity is realized compared with the free H_3TTTA and 2,2-bpy ligands, of which the former shows very weak luminescence while the latter exhibits emissions at both 365 and 385 nm [54]. The intensity increase blue- or red-shift of the luminescence may be attributed to the chelation of the ligand to the metal center, which increases the rigidity of ligand and reduces the nonradiative relaxation process [55–57]. For further verification based on the experimental geometries, the MO calculations of the binuclear complexes **2** and **3** have been carried out (Fig. 8). The contour plots of the relevant HOMOs and LUMOs for these two complexes show large difference. For complex **2**, the HOMO is mainly associated with the π-bonding orbital from the triazine rings and S atoms of the TTTA ligands, while the LUMO is mainly associated with the π^*-antibonding orbital from the bpy rings. For complex **3**, however, both HOMO and LUMO are mainly associated with the Cd–O and Cd–N σ-bonding orbital around the metal centers, which is localized more on the N and O atoms, respectively.

3.3.3. Magnetic properties

The thermal dependence of $\chi_M T$ and the simulated curves for polycrystalline samples of complex **6** are shown in Fig. 9. The value of $\chi_M T$ was 12.45 $cm^3\ mol^{-1}\ K$ at 300 K, slightly smaller than the value for three isolated $S=5/2$ Mn^{II} center (13.125 $cm^3\ mol^{-1}\ K$), which might be caused by the weak antiferromagnetic coupling between the metal centers. The $\chi_M T$ values decrease steadily with the decreasing temperature. Below 50 K, the value decreases dramatically and reached 4.37 $cm^3\ mol^{-1}\ K$ at 1.8 K, consistent with the resulting spin ground state of $S=5/2$ and further indicating the antiferromagnetic interaction between the Mn^{II} ions.

An inspection of the structure of the complex allows us to account for the observed antiferromagnetic coupling. Because of the long metal–metal distance between the metal centers of different trinuclear SBUs, only the coupling interactions between the metal centers within them are considered. For the triply bridged metals, each bridge contributes to the coupling between the metal centers. Firstly, two carboxylate groups bridge the metal centers in *syn–syn* fashion, which always leads to possible antiferromagnetic interactions [58,59]; secondly, for the η^2–O bridge, the magnetic coupling between the metal centers depends on the Mn–O–Mn angle to a large extent. The Mn–O–Mn angle of 105.5(1)° may also lead to antiferromagnetic exchange interactions [60,61].

In order to evaluate the exchange interactions between neighboring Mn(II) centers, the susceptibility measurements were fitted in all temperature region assuming the isotropic spin-coupling Hamiltonian $H=-2J(S_1\cdot S_2+S_{1A}\cdot S_2)$ [62]. The best fits with the parameters of $g=1.99$ and $J=-1.44\ cm^{-1}$ are consistent with other reported values of similar structures [63,64].

4. Conclusions

Six complexes based on a flexible tripodal ligand H_3TTTA have been hydrothermally synthesized and structurally characterized. They exhibit diverse structures from discrete mono- and binuclear molecules to extended two-dimensional layers. pH of the

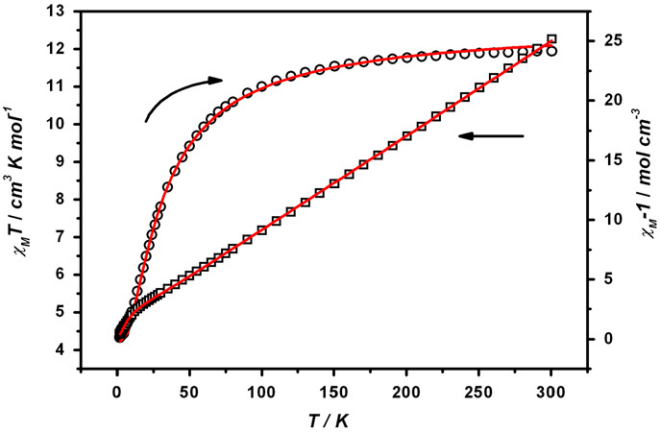

Fig. 9. Magnetic behavior of **6** in the form of $\chi_M T$ vs. T and χ_M^{-1} vs. T plots for complex **6**. The solid line shows the best fit.

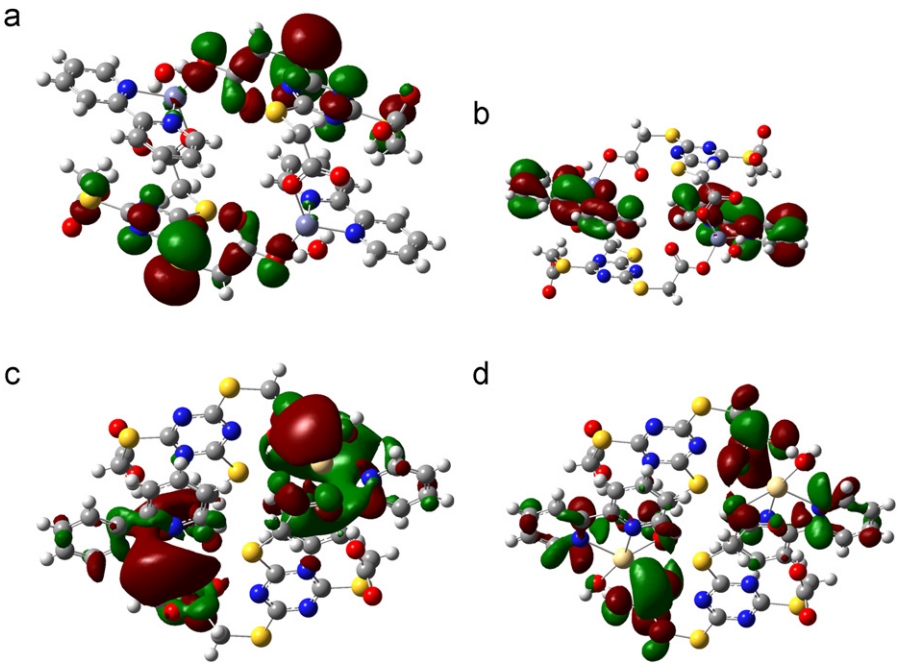

Fig. 8. The contour plots of the relevant LUMOs and HOMOs for **2** (a and b) and **3** (c and d), respectively.

reaction system and the metal ions has large influence on the final products. The flexible multicarboxylic acid ligand exhibits diverse different coordination modes ranging from monodentate to μ^6-bridge. These special structures may enrich the frameworks of multicarboxylate system to some extent.

Supporting information available

Additional figures of complex 3 and crystallographic data for all the complexes. These data can be obtained free of charge via 〈http://www.ccdc.cam.ac.uk/conts/retrieving.html〉 or from the Cambridge Crystallographic Data Centre, 12 Union Road, Cambridge CB2 1EZ, UK; fax: (+44) 1223-336-033; or e-mail: deposit@ccdc.cam.ac.uk.

Acknowledgments

We gratefully acknowledge financial support from the National Natural Science Foundation of China (Grant no. 20801025) and Shandong Taishan Scholar Fund.

Appendix A. Supplementary material

Supplementary data associated with this article can be found in the online version at doi:10.1016/j.jssc.2011.04.029.

References

[1] J.M. Lehn, Supramolecular Chemistry: Concepts and Perspectives, VCH, Weinheim, 1995.
[2] J.M. Lehn, J.L. Atwood, E.D.J. Davis, D.D. MacNicol, F. Vögtle (Eds.), Comprehensive Supramolecular Chemistry, vols. 1–11, Pergamon, Oxford, 1990–1996.
[3] P.J. Stang, B. Olenyuk, Acc. Chem. Res. 30 (1997) 502.
[4] S.R. Batten, CrystEngComm 3 (2001) 67.
[5] L. Carlucci, G. Ciani, D.M. Proserpio, Coord. Chem. Rev. 246 (2003) 247.
[6] C. Janiak, J. Chem. Soc., Dalton Trans. (2003) 2781.
[7] S. Kitagawa, R. Kitaura, S. Noro, Angew. Chem. Int. Ed. 43 (2004) 2334.
[8] C.N.R. Rao, S. Natarajan, R. Vaidhyanathan, Angew. Chem. Int. Ed. 43 (2004) 1466.
[9] G. Ferey, C. Mellot-Draznieks, C. Serre, F. Millange, Acc. Chem. Res. 38 (2005) 217.
[10] S. Kitagawa, S. Noro, T. Nakamura, Chem. Commun. (2006) 701.
[11] J.P. Zhang, X.M. Chen, Chem. Commun. (2006) 1689.
[12] G. Ferey, C. Serre, Chem. Soc. Rev. 38 (2009) 1380.
[13] J.R. Long, O.M. Yaghi, Chem. Soc. Rev. 38 (2009) 1213.
[14] L.J. Murray, M. Dinc, J.R. Long, Chem. Soc. Rev. 38 (2009) 1294.
[15] T. Uemura, N. Yanai, S. Kitagawa, Chem. Soc. Rev. 38 (2009) 1228.
[16] J.P. Zhang, X.C. Huang, X.M. Chen, Coord. Soc. Rev. 38 (2009) 2385.
[17] L. Pan, B. Parker, X.Y. Huang, D.H. Oison, J.Y. Lee, J.J. Li, Am. Chem. Soc. 128 (2006) 4180.
[18] H. Chun, H. Jung, Inorg. Chem. 48 (2009) 417.
[19] L. Xu, S.H. Yan, E.Y. Choi, J.Y. Lee, Y.U. Kwon, Chem. Commun. (2009) 3431.
[20] A. Lan, K.H. Li, H.H. Wu, L.Z. Kong, N. Nijem, D.H. Olson, T.J. Emge, Y.J. Chabal, D.C. Langerth, M.C. Hong, J. Li, Inorg. Chem. 48 (2009) 7165.
[21] Y.J. Kim, M. Suh, D.Y. Jung, Inorg. Chem. 43 (2004) 245.
[22] H.F. Zhu, Z.H. Zhang, T.A. Okamura, W.Y. Sun, N. Ueyama, Cryst. Growth Des. 5 (2005) 177.
[23] J. Wang, Y.H. Zhang, M.L. Tong, Chem. Commun. (2006) 3166.
[24] S.Q. Zang, Y. Su, Y.Z. Li, Z.P. Ni, H.Z. Zhu, Q.J. Meng, Inorg. Chem. 45 (2006) 3855.
[25] S.Q. Ma, J.M. Simmons, D.F. Sun, A.Q. Yuan, H.C. Zhou, Inorg. Chem. 48 (2009) 5263.
[26] S.T. Wu, L.Q. Ma, L.S. Long, L.S. Zheng, W.B. Lin, Inorg. Chem. 48 (2009) 2436.
[27] Y. Ma, A.L. Cheng, E.Q. Gao, Cryst. Growth. Des. 10 (2010) 2832.
[28] I. Goldberg, Chem. Commun. (2005) 1243 and references therein.
[29] S. Varughese, V.R. Pedireddi, Chem. Commun. (2005) 1824.
[30] M. Dan, A.K. Cheetham, C.N.R. Rao, Inorg. Chem. 45 (2006) 8227.
[31] K. Uemura, K. Saito, S. Kitagawa, H. Kita, J. Am. Chem. Soc. 128 (2006) 16122.
[32] S.N. Wang, Y. Yang, J.F. Bai, Y.Z. Li, M. Scheer, Y. Pan, X.Z. You, Chem. Commun. (2007) 4416.
[33] Q. Yue, X.B. Qian, L. Yan, E.Q. Gao, Inorg. Chem. Commun. (2008) 1067.
[34] W. Wei, M.Y. Wu, Q. Gao, Q.F. Zhang, Y.G. Huang, F.L. Jiang, M.C. Hong, Inorg. Chem. 48 (2009) 420.
[35] D.R. Turner, S.N. Pek, S.R. Battern, CrystEngComm (2009) 87.
[36] X.J. Jiang, S.Z. Zhang, J.H. Guo, X.G. Wang, J.S. Li, M. Du, CrystEngComm (2009) 855.
[37] S.N. Wang, H. Xing, Y.Z. Li, J. Bai, Y. Pan, M. Scheer, X.Z. You, Eur. J. Inorg. Chem. (2006) 3041.
[38] R. Sun, S.N. Wang, H. Xing, J. Bai, Y.Z. Li, Y. Pan, X.Z. You, Inorg. Chem. 46 (2007) 8451.
[39] S.N. Wang, H. Xing, J. Bai, Y.Z. Li, Y. Pan, M. Scheer, X.Z. You, Chem. Commun. (2007) 2293.
[40] T.Y. Min, B. Zheng, J.F. Bai, R. Sun, Y.Z. Li, Z.X. Zhang, CrystEngComm 12 (2010) 70.
[41] S.N. Wang, R. Sun, X.S. Wang, Y.Z. Li, Y. Pan, J. Bai, M. Scheer, X.Z. You, CrystEngComm 9 (2007) 1051.
[42] G.M. Sheldrick, SHELXS-97, Program for Crystal Structure Solution, Göttingen University, Göttingen, Germany, 1997;
G.M. Sheldrick, SHELXL-97, Program for Crystal Structure Refinement, Göttingen University, Göttingen, Germany, 1997.
[43] A.F. Wells, Structural Inorganic Chemistry, 4th ed., Clarendon Oxford University Press, New York, 1975.
[44] H. Chun, D. Kim, D.N. Dybtsev, K. Kim, Angew. Chem. Int. Ed. 43 (2004) 971.
[45] N.W. Ockwig, O. Delgado-Friedrichs, M. OUKeeffe, O.M. Yaghi, Acc. Chem. Res. 38 (2005) 176.
[46] R. Natarajan, G. Savitha, P. Dominiak, K. Wozniak, J.N. Moorthy, Angew. Chem. Int. Ed. 44 (2005) 2115.
[47] M. Du, Z.H. Zhang, X.-J. Zhao, Q. Xu, Inorg. Chem. 45 (2006) 5785.
[48] 〈http://www.chem.monash.edu.au/staff/sbatten/interpen/index.html〉.
[49] I.A. Baburin, V.A. Blatov, L. Carlucci, G. Ciani, D.M. Proserpio, J. Solid State Chem. 178 (2005) 2452.
[50] M. Du, Z.H. Zhang, L.F. Tang, X.G. Wang, X.J. Zhao, S. R. Batten, Chem. Eur. J 13 (2007) 2578.
[51] X.J. Jiang, M. Du, Y. Sun, J.H. Guo, J.S. Li, J. Solid State Chem. 182 (2009) 3211.
[52] R.H. Wang, M.C. Hong, J.H. Luo, R. Cao, J.B. Weng, Chem. Commun. (2003) 1018.
[53] L. Chen, G.J. Xu, K.Z. Shao, Y.H. Zhao, G.S. yang, Y.Q. Lan, X.L. Wang, H.B. Xu, Z.M. Su, CrystEngComm 12 (2010) 2157.
[54] R.X. Yuan, R.G. Xiong, Y.L. Xie, X.Z. You, S.M. Peng, G.H. Lee, Inorg. Chem. Commun. 4 (2001) 384.
[55] X.L. Wang, C. Qin, E.B. Wang, L. Xu, Z.M. Su, C.W. Hu, Angew. Chem. Int. Ed. 43 (2004) 5036.
[56] J. Zhang, Y.R. Xie, Q. Ye, R.G. Xiong, Z.L. Xue, X.Z. You, Eur. J. Inorg. Chem. (2003) 2572.
[57] S.L. Zheng, J.H. Yang, X.L. Yu, X.M. Chen, W.T. Wong, Inorg. Chem. 43 (2004) 830.
[58] A. Escuer, E. Peñlba, R. Vicente, X. Solans, M.J. Font-Badía, J. Chem. Soc. Dalton Trans. (1997) 2315.
[59] M. Rodríguez, A. LLobet, M. Corbella, P. Müller, M.A. Usón, A.E. Martell, J. Reibenspens, J. Chem. Soc. Dalton Trans. (2002) 2900.
[60] H.L. Shyu, H.H. Wei, Y. Wang, Inorg. Chim. Acta 290 (1999) 8.
[61] S. Saha, D. Mal, S. Koner, A. Bhattacherjee, P. Gutlich, S. Mondal, M. Mukherjee, K.I. Okamoto, Polyhedron 23 (2004) 1811.
[62] R.L. Carlin, Magnetochemistry, Springer, New York, 1983.
[63] V. Tangoulis, D.A. Malamatari, K. Soulti, V. Stergiou, C.P. Raptopoulou, A. Terzis, T.A. Kabanos, D.P. Kessissoglou, Inorg. Chem. 35 (1996) 4974.
[64] C.J. Milios, T.C. Stamatatos, P. Kyritsis, A. Terzis, C.P. Raptopoulou, R. Vicente, A. Escuer, S.P. Perlepes, Eur. J. Inorg. Chem. (2004) 2885.